Improved Dynamic Model of Fast-Settling Linear-in-dB Automatic Gain Control Circuit

Hsuan-Yu Marcus Pan and Lawrence E. Larson
University of California, San Diego
9500 Gilman Drive
La Jolla, CA, 92093, USA
hspan@ucsd.edu

***Abstract*—An improved exact dynamic model of a fast-settling linear-in-dB Automatic Gain Control (AGC) circuit is proposed. The explicit transient behavior is calculated for a first-order and second-order AGC loop.**

I. Introduction

Automatic Gain Control (AGC) circuits are used in many systems, where the input amplitude varies over a wide dynamic range and the output amplitude is designed to achieve a certain specified level. An AGC circuit is usually composed of a peak detector (PD), a variable gain amplifier (VGA), and a loop filter, as shown in Fig.1 [1]. The output of the VGA is detected by the peak detector, and compared with a reference voltage V_{ref}. Since the gain of the VGA is adjusted according to the amplitude of the input, the resulting output amplitude is constant.

AGC circuits can be categorized according to different gain characteristics of the VGA. One of the most popular types is the "Linear-in-dB" VGA, whose gain control has an exponential characteristic [2]. As a result of this characteristic, an exact analysis of the large-signal settling behavior of the Linear-in-dB circuit is very difficult. Previous authors have used a Taylor series expansion to approximate the exponential function in the overall loop analysis [1, 3-4], which is only valid for small input level variations. One important use of this VGA is as a feedback control element for a wideband polar transmitter [5-6]. These circuits require a very wide dynamic range for their operation and therefore an exact analysis of the settling behavior of the Linear-in-dB VGA is needed.

In light of this, we present an exact dynamic large-signal model of a linear-in-dB AGC circuit. Our proposed model is capable of describing the entire loop large-signal behavior, and exactly predicts the overall loop settling time dependence on input amplitude variations.

The paper is organized as follows: Section II reviews the AGC loop operation and derives the first-order exact steady-state large signal model. Section III generalizes the analysis to a second-order response. Section IV derives the settling time of the overall loop. Section V compares the calculated settling time results with behavioral simulation results. Conclusions are provided in Section VI.

II. AGC Circuit Operation and First-Order Steady-State Large Signal Modeling

A. *First-order Steady-state Large-signal Model*

The first-order basic AGC loop is shown in Fig.1. According to the linear-in-dB operation of the VGA, the output of the VGA can be expressed as:

$$V_{out} = V_{in} \times \alpha \times e^{V_{ctrl}/V_T} \tag{1}$$

where α is the VGA gain when the control voltage V_{ctrl} is zero, and V_T is the constant representing the linear-in-dB slope.

As an example, suppose an envelope-modulated signal is fed to the input of the VGA, V_{in} can be written as

$$V_{in} = A\,(1 + m\cos\omega_e t)\cos\omega_c t \tag{2}$$

where m is the modulation index of the envelope-modulated signal, ω_e is the envelope angular frequency and ω_c is the carrier angular frequency [7, 8].

Based on peak extraction operation, the output of the peak detector V_{pd} can be expressed as

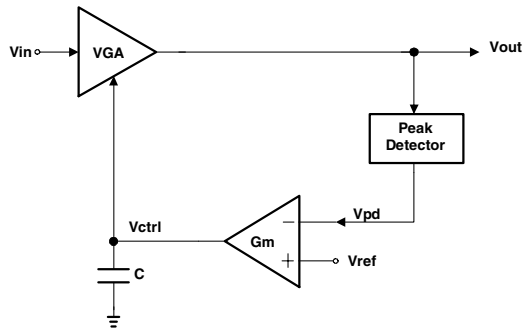

Fig.1. Basic AGC circuit block diagram. The gain of VGA is adjusted according to the amplitude of V_{in} to hold V_{out} at constant-amplitude.

$$V_{pd} = Peak(V_{out}) \tag{3}$$

where *Peak( )* is the peak extraction function. The output of the g_m-C filter, which acts as a loop filter, can also be described as

$$V_{ctrl} = \frac{1}{C}\int_{-\infty}^{t} g_m(V_{ref} - V_{pd})dt \tag{4}$$

where V_{ctrl} is integrated from the error term V_{ref}-V_{pd}.

Combining (1)-(4), we have

$$\frac{dV_{ctrl}}{dt} = \frac{g_m}{C}(V_{ref} - A\ (1 + m\cos\omega_e t)\times\alpha\times e^{V_{ctrl}/V_T}) \tag{5}$$

Equation (5) describes the transient behavior of V_{ctrl} of the first-order AGC circuit. It is a nonlinear first-order differential equation and is difficult to solve directly. However, (5) can be simplified by substituting $u = e^{V_{ctrl}/V_T}$ and then:

$$\frac{1}{u^2}\frac{du}{dt} - \frac{g_m}{C}\frac{V_{ref}}{V_T}\frac{1}{u} = -\frac{g_m}{C}\frac{A\times\alpha(1+m\cos\omega_e t)}{V_T} \tag{6}$$

Equation (6) is known as the Bernoulli Equation [9] and can be solved as

$$u = \left(\frac{\omega_{gm}A\times\alpha}{V_T}\frac{m\cos(\omega_e t-\phi)}{\sqrt{\omega_e^2+\left(\frac{\omega_{gm}V_{ref}}{V_T}\right)^2}} + \frac{A\alpha}{V_{ref}} + Pe^{-\frac{\omega_{gm}V_{ref}}{V_T}t}\right)^{-1} \tag{7}$$

where $\phi = \tan^{-1}\frac{CV_T\omega_e}{g_m V_{ref}}$, $\omega_{gm} = \frac{g_m}{C}$ and P is the integration constant.

Finally, the control voltage V_{ctrl} can be obtained by applying $V_{ctrl} = V_T \ln u$ and solved explicitly as

$$V_{ctrl} = -V_T \ln\left[\frac{\omega_{gm}A\times\alpha}{V_T}\frac{m\cos(\omega_e t-\phi)}{\sqrt{\omega_e^2+\left(\frac{\omega_{gm}V_{ref}}{V_T}\right)^2}} + \frac{A\alpha}{V_{ref}} + Pe^{-\frac{\omega_{gm}V_{ref}}{V_T}t}\right] \tag{8}$$

B. First-order Steady-state Behavior

In steady state, the $Pe^{-\frac{\omega_{gm}V_{ref}}{V_T}t}$ term in (8) can be neglected and V_{out} can also be solved explicitly by combining and substituting V_{ctrl} of (8) into (1) and (3).

$$V_{out,ss1} = \frac{(1+m\cos\omega_e t)}{1+\frac{m\cos(\omega_e t-\phi)}{\sqrt{\left(\frac{\omega_e V_T}{\omega_{gm}V_{ref}}\right)^2+1}}}V_{ref}\cos\omega_c t \tag{9}$$

If ω_e is relatively small when compared with $\omega_{gm}V_{ref}/V_T$, the envelope of $V_{out,ss1}$ can be approximated to V_{ref} (steady-state value), which means the overall AGC can settle within a very short time. If ω_e is large, (9) implies that the AGC cannot keep the output amplitude constant.

II. AGC Circuit Second-Order Large Signal Model

A. Peak Detector Delay Model

The analysis in the previous section was concerned only with the first-order (single-pole) approximation, where the pole is only determined by the g_m-C filter and there are no delays anywhere else in the circuit. However, as the input frequency increases, other poles in the circuit become more important [10]. Therefore, a second-order large-signal model is proposed here, which takes into account the other poles associated with the peak detector.

Consider the peak detector delay model in Fig. 2, where the input signal is $A\cos(\omega t)$ and ω_p is the angular frequency of the associated pole. In steady state, the output of the peak detector delay block, $V_{dout}(t)$, can be calculated by the Inverse Laplace Transform of $V_{dout}(s)$ as follows:

$$V_{dout}(t) = \frac{A\omega_p}{\sqrt{\omega^2+\omega_p^2}}\cos(\omega t-\varphi_d), \phi_d = \tan^{-1}\left(\frac{\omega}{\omega_p}\right) \tag{10}$$

B. Second-order Steady-state Behavior

If we insert the above delay block between the output of the PD and the input to g_m-C filter to model the delay associated with the PD, as shown in Fig. 3, the input of g_m-C filter can be calculated by combining (2) and (3), and be re-written as

$$V_{gmc} = A\alpha e^{vctrl/V_T}\left[u(t) - e^{-\omega_p t} + \frac{m\omega_p\cos(\omega_e t-\varphi_d)}{\sqrt{\omega_e^2+\omega_p^2}}\right] \tag{11}$$

In steady state, the $e^{-\omega_p t}$ term can be ignored. By substituting V_{pd} with V_{gmc} and solving (1), (2), (4), and (11), the steady-state value of V_{ctrl} can be obtained as:

$$V_{ctrl,ss2} = -V_T \ln\left\{\frac{\frac{\omega_{gm}\omega_p mA\alpha}{\omega_e V_T\sqrt{\omega_e^2+\omega_p^2}}[\cos(\omega_e t-\varphi_t)]}{\sqrt{\left[\frac{\omega_{gm}V_{ref}}{\omega_e V_T}\right]^2+1}} + \frac{A\alpha}{V_{ref}}\right\} \tag{12}$$

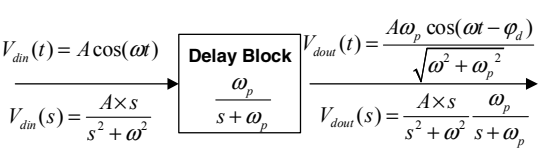

Fig.2. Peak detector delay block diagram.

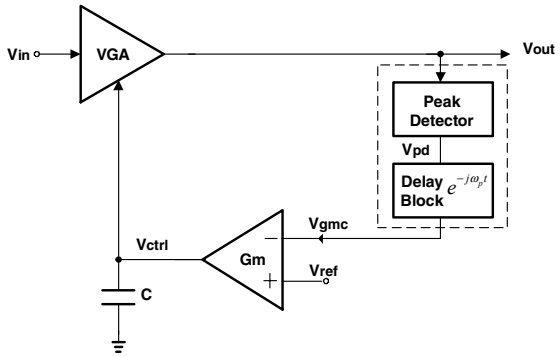

Fig.3. Second-order AGC circuit block diagram. The dotted area represents the new peak detector model including the delay of the peak detector.

where $\varphi_t = \tan^{-1}\frac{\omega_e V_T}{\omega_{gm} V_{ref}} + \tan^{-1}(\frac{\omega_e}{\omega_p})$. When ω_p is much greater than ω_e, (12) reduces to (8) as expected.

In a similar manner to Section II, V_{out} and V_{pd} can also be expressed explicitly by combining and substituting V_{ctrl} of (12) into (1) and (3). Equation (12) also shows that the loop's overall response could be severely impeded by a low ω_e (corresponding to excessive loop delay). To validate our theory, the V_{pd} root mean square error percentage with respect to (ω_e/ω_p), from SPICE simulation and calculation, is shown in Fig. 4. It can be seen that the error percentage increases when (ω_e/ω_p) increases, and calculation and simulation results agree closely.

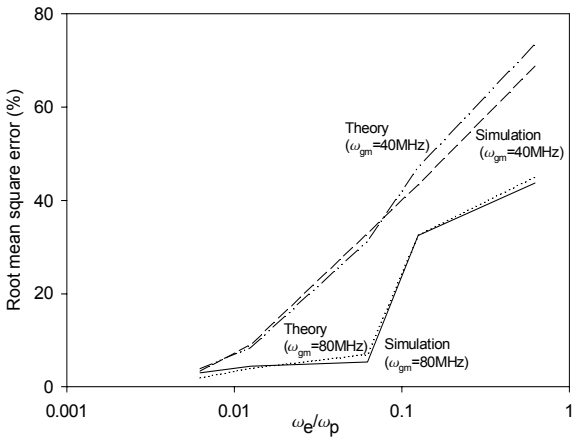

Fig.4. Second-order AGC circuit root mean square error percentage vs. (ω_e/ω_p) from SPICE simulation and theory . The error percentage increases when ω_e increases. Simulation parameters: V_T=0.6V, ω_c=2GHz, V_{ref}=0.24V, A=1mV, g_m=0.5mS and 1mS, C=2pF, α=0.1, m=0.9.

III. AGC Loop Settling time

A. First-order AGC Circuit Settling Time Calculation

Specifications for an AGC circuit often involve certain requirements associated with the transient response, and one important figure-of-merit is the settling time [3]. A simple way of measuring this is to apply a unit step response to the system, i.e.

$$V_{in} = A_1(1 + k \times u(t))\cos\omega_c t \tag{13}$$

Where $u(t)$ is the unit-step function and k is the input amplitude variation factor. The first-order V_{ctrl} transient response with respect to input unit-step response is

$$V_{ctrl,sr1} = V_T\left[\ln(\frac{V_{ref}}{A_1(1+k)\alpha}) - \ln(1-(\frac{k}{1+k})e^{-(\frac{\omega_{gm}V_{ref}}{V_T}t)})\right] \tag{14}$$

and V_{out} can be solved by substituting (14) into (1)

$$V_{out,sr1} = \frac{V_{ref}\cos\omega_c t}{1-(\frac{k}{1+k})e^{-(\frac{\omega_{gm}V_{ref}}{V_T}t)}} \tag{15}$$

Then the 1% settling time T_s [12] of the $V_{out,sr1}$'s envelope can be solved as

$$T_s = \frac{V_T}{\omega_{gm}V_{ref}}\ln\left[\frac{k+100}{k+1}\right] \tag{16}$$

Not surprisingly, (16) shows that the settling time is not only a function of $\omega_{gm}V_{ref}/V_T$, but also a function of input amplitude variation ratio k.

B. Second-order AGC Circuit Settling Time Calculation

Similarly, the second-order AGC circuit settling time can also be calculated by applying a unit step response to the circuit in Fig.3. The second-order V_{ctrl} transient response with respect to input unit-step response can be shown as follows:

$$V_{ctrl,sr2}(t) = V_T\ln\left[\frac{\frac{V_{ref}}{A_1\alpha(1+k)}}{\left[1+\frac{e^{-\omega_p t}}{\frac{\omega_p V_T}{\omega_{gm}V_{ref}}-1}-\left(\frac{\frac{\omega_p V_T}{\omega_{gm}V_{ref}}}{\frac{\omega_p V_T}{\omega_{gm}V_{ref}}-1}-\frac{1}{1+k}\right)e^{\frac{V_{ref}\omega_{gm}}{V_T}t}\right]}\right] \tag{17}$$

where ω_p represents the pole angular frequency of peak detector. Substituting (17) into (1) and (3), the envelope of V_{out}, V_{pd} , then becomes

$$V_{pd,sr2}(t) = \frac{V_{ref}}{\left[1 + \frac{e^{-\omega_p t}}{\frac{\omega_p V_T}{\omega_{gm} V_{ref}} - 1} - \left(\frac{\frac{\omega_p V_T}{\omega_{gm} V_{ref}}}{\frac{\omega_p V_T}{\omega_{gm} V_{ref}} - 1} - \frac{1}{1+k}\right) e^{-\frac{V_{ref}\omega_{gm}}{V_T} t}\right]} \quad (18)$$

The settling time T_s is difficult to be expressed explicitly from (18) but it can be solved iteratively. Equation (18) shows that the transient behavior is a function of $\omega_{gm} V_{ref} / V_T$, input amplitude variation ratio k and peak detector pole ω_p. If ω_p is very low, the V_{pd} settling response is dominated by ω_p rather than $\omega_{gm} V_{ref} / V_T$. Therefore, to achieve a fast settling AGC circuit, it is important to increase ω_p [13], ω_{gm}, and the ratio V_{ref}/V_T.

IV. AGC Simulations and Verification of Analysis

Behavioral level simulations are provided in this section to compare the first-order/second-order settling time simulation results and theoretical results, where the second-order settling time is calculated iteratively. The response of the AGC circuit is shown in Fig. 5, where previous theories [1, 3-4] did not describe the loop characteristics dependence on input amplitude variation ratio k. Note that the first-order estimation is only valid for small (ω_e/ω_p) ratio .The theoretical calculation results predicted by our theory are close to SPICE behavioral level simulation results.

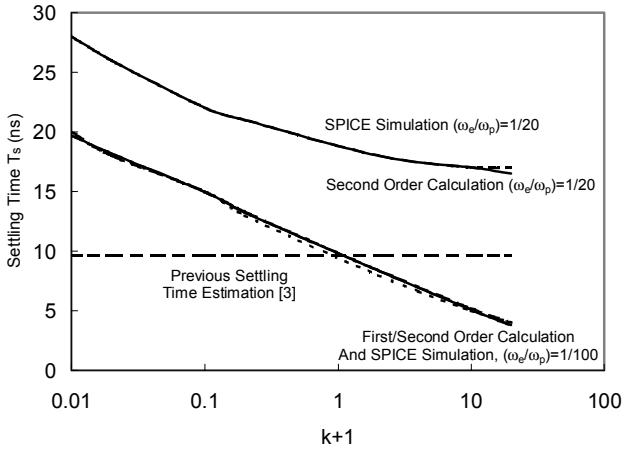

Fig.5. Comparison of first-order and second-order AGC circuit settling time simulation and calculation results for (ω_e/ω_p)=1/20 and 1/100. Settling time T_s is a function of input amplitude variation ratio k. Simulation parameters: V_T=0.6V, ω_t=2GHz, V_{ref}=0.24V, A=1mV, g_m=1mS, C=2pF, α=0.1, m=0.9.

V. Conclusion

An exact dynamic model of linear-in-dB Automatic Gain Control (AGC) circuit is proposed and validated. The explicit steady-state behavior and the overall loop settling time are calculated for first-order and second-order AGC loops. The analysis shows that the overall loop settling time depends on the input amplitude ratio, phase detector delay, and other loop parameters. This exact large-signal model can also be used for the design of wideband closed-loop polar transmitters.

References

[1] P. Huang, C. Huang and C. K. Wang, "A 155-MHz BiCMOS automatic gain control amplifier," IEEE Transactions of Circuits and Systems II, Analog and Digital Signal Processing, Vol. 46, Issue 5, May 1999, pp. 643-647.

[2] S. Otaka, G. Takemura and H. Tanimoto, "A low-power low-noise accurate linear-in-dB variable-gain amplifier with 500-MHz bandwidth," IEEE Journal of Solid-State Circuits, Vol.35, Issue, 12, Dec. 2000, pp.1942-1948.

[3] J. Khoury, "On the design of constant settling time AGC Circuits," IEEE Transactions of Circuits and Systems, II: Analog and Digital Signal Processing, Vol. 45, Issue 3, March 1998, pp. 282-294.

[4] M. Shiue , K.H. Huang, C. C. Lu, C. K. Wang, and W. I. Way, "A VLSI design of dual-loop automatic gain control for dual-mode QAM/VSB CATV modem," IEEE ISCAS'98 Symposium Digest, June 1998, pp.490-493.

[5] M. Ito, T. Tamawaki, M. Kasahara and S. Williams, "Variable gain amplifier in polar loop modulation transmitter for EDGE," Proceeding of ESSCIRC 2005, Sept 2005, pp. 511-514.

[6] T. Sowlati, D. Rozenblit, R. Pullela, M. Damgaard, E. McCarthy and D. Koh etal, "Quad-Band GSM/GPRS/EDGE polar transmitter," IEEE Journal of Solid-State Circuits, Vol. 39, No.12, Dec. 2004, pp. 2179-2189.

[7] T. H. Lee, *The Design of CMOS Radio-Frequency Integrated Circuits*, Cambridge University Press, 2nd Edition, 2004, p.60-64.

[8] R. E. Ziemer and W. H. Tranter, *Principle of Communication*, 5th edition,, John Wiely & Son Inc., 2002, pp. 106-124.

[9] P. V. O'Neil, *Advanced Engineering Mathematics*, PWS-KENT Publishing Company, 4th Editon, 1995, pp.40-43.

[10] P. R. Gray, P. J. Hurst, S. H. Lewis and R. G. Meyer, *Analysis and Design of Analog Integrated Circuits*, 4th editon, John Wiely & Son Inc., 2001, pp.488-552.

[11] P. V. O'Neil, *Advanced Engineering Mathematics*, PWS-KENT Publishing Company, 4th Editon, 1995, pp.115-158.

[12] G. F. Franklin, J. D. Powell and A. E. Naeini, *Feedback Control of Dyamic Systems*, Addison-Wesley Publishing Company, 3rd edition, 1994, pp. 85-165.

[13] E. A. Grain and M. Perrott, "A 3.125 Gb/s limiting amplifier in CMOS with 42dB gain and 1μs offset compensation," IEEE Journal of Solid-State Circuits, Vol.41, No.2, Feb 2006, pp.443-451.